

Identification of ASYNAPTIC4, a Component of the Meiotic Chromosome Axis

Chambon, Aurélie; West, Allan; Vezon, Daniel; Horlow, Christine; De Muyt, Arnaud; Chelysheva, Liudmila; Ronceret, Arnaud; Darbyshire, Alice; Osman, Kim; Heckmann, Stefan; Franklin, F Chris H; Grelon, Mathilde

DOI:
[10.1104/pp.17.01725](https://doi.org/10.1104/pp.17.01725)

License:
None: All rights reserved

Document Version
Peer reviewed version

Citation for published version (Harvard):
Chambon, A, West, A, Vezon, D, Horlow, C, De Muyt, A, Chelysheva, L, Ronceret, A, Darbyshire, A, Osman, K, Heckmann, S, Franklin, FCH & Grelon, M 2018, 'Identification of ASYNAPTIC4, a Component of the Meiotic Chromosome Axis', *Plant Physiology*, vol. 178, no. 1, pp. 233-246. <https://doi.org/10.1104/pp.17.01725>

[Link to publication on Research at Birmingham portal](#)

Publisher Rights Statement:
Checked for eligibility 15/10/2018

First published in *Plant Physiology*
<https://doi.org/10.1104/pp.17.01725>

General rights

Unless a licence is specified above, all rights (including copyright and moral rights) in this document are retained by the authors and/or the copyright holders. The express permission of the copyright holder must be obtained for any use of this material other than for purposes permitted by law.

- Users may freely distribute the URL that is used to identify this publication.
- Users may download and/or print one copy of the publication from the University of Birmingham research portal for the purpose of private study or non-commercial research.
- User may use extracts from the document in line with the concept of 'fair dealing' under the Copyright, Designs and Patents Act 1988 (?)
- Users may not further distribute the material nor use it for the purposes of commercial gain.

Where a licence is displayed above, please note the terms and conditions of the licence govern your use of this document.

When citing, please reference the published version.

Take down policy

While the University of Birmingham exercises care and attention in making items available there are rare occasions when an item has been uploaded in error or has been deemed to be commercially or otherwise sensitive.

If you believe that this is the case for this document, please contact UBIRA@lists.bham.ac.uk providing details and we will remove access to the work immediately and investigate.

1 Short Title: ASY4, a new meiotic chromosome axis component

2

3 Corresponding author: Mathilde Grelon

4

5 Identification of a new component of the meiotic chromosome axis in *Arabidopsis*
6 *thaliana*

7

8 Aurélie Chambon¹, Allan West², Daniel Vezon¹, Christine Horlow¹, Arnaud De Muyt¹,
9 Liudmila Chelysheva¹, Arnaud Ronceret¹, Alice Darbyshire², Kim Osman², Stefan
10 Heckmann², F. Chris. H. Franklin², Mathilde Grelon¹

11

12 ¹Institut Jean-Pierre Bourgin, INRA, AgroParisTech, CNRS, Université Paris-Saclay,
13 RD10, 78026 Versailles Cedex, France

14

15 ²School of Biosciences, University of Birmingham, Edgbaston, Birmingham, United
16 Kingdom

17

18

19 **Abstract:**

20 During the leptotene stage of prophase I of meiosis chromatids become organized
21 into a linear looped array by a protein axis that forms along the loop bases.
22 Establishment of the axis is essential for the subsequent synapsis of the homologous
23 chromosome pairs and the progression of recombination to form genetic crossovers.
24 Here we describe ASY4 a new component of the meiotic protein axis in *Arabidopsis*
25 *thaliana*. ASY4 is a small coil-coiled protein that exhibits limited homology with the C-
26 terminal region of the axis protein ASY3. We show using an eYFP-tagged ASY4 that
27 the protein localizes to the chromosome axis throughout prophase I. Bi-molecular
28 fluorescence reveals that ASY4 interacts with ASY1 and ASY3 and yeast two-hybrid
29 analysis confirms a direct interaction between ASY4 and ASY3. Mutants lacking full-
30 length ASY4 exhibit defective axis formation and are unable to complete synapsis.
31 Although initiation of recombination appears unaffected in an *asy4* mutant,
32 crossovers are significantly reduced and tend to group in the distal parts of the
33 chromosomes. In summary, we have identified a new component of the meiotic
34 chromosome axis that is required for normal axis formation and controlled crossover
35 formation.

36

37

38

39 **Introduction**

40

41 Meiosis is the specialised cell division that generates the haploid cells from which the
42 gametes will be generated. In most organisms this ploidy reduction is achieved by
43 segregating, first, the homologous chromosomes from each other (meiosis I), then,
44 by separating the sister chromatids at meiosis II. The correct meiotic course relies on
45 a series of coordinated mechanisms that take place during meiotic prophase I. They
46 include the organisation of sister chromatids along a common proteinaceous axis
47 (the axial element, AE), the pairing and the synapsis of these axes, recombination
48 and the formation of at least one crossover (CO) per homologous pair (Zickler and
49 Kleckner, 1999).

50

51 The AEs are assembled early during meiotic prophase I, defining the leptotene stage.
52 Then, axes from the homologous chromosomes become connected by the
53 polymerisation of the central element of the synaptonemal complex (SC), forming the
54 lateral elements (LEs) of the SC. The polymerisation of the SC is complete by
55 pachytene, a stage at which the maturation of recombination intermediates into COs
56 is achieved, at least in *S. cerevisiae* (Zickler and Kleckner, 1999). Next, the central
57 element of the SC is disassembled while the chromosome axis participates in the
58 dramatic chromosome condensation that occurs during the remaining steps of
59 meiotic prophase I (diplotene, diakinesis).

60

61 Therefore, a defining feature of meiotic chromosomes is that sister chromatids share
62 a chromosome axis to which they are anchored, forming regular arrays of chromatin
63 loops. Because most of the recombination proteins are axis-associated, it has been
64 proposed that meiotic chromosome axes form a scaffold on which meiotic
65 recombination takes place (Blat et al., 2002; Panizza et al., 2011). Notwithstanding
66 these structural roles, chromosome axes also appear highly flexible and dynamic.
67 Their physical association with the chromosomes depends on and is responsive to
68 underlying transcriptional activity (Sun et al., 2015). Some of their components are
69 displaced upon synapsis and during recombination, where there is a requirement for
70 localized axis exchange at CO sites.

71

72 Chromosome axes are composed of various protein families (Zickler and Kleckner,
73 1999). Cohesins (and notably the meiosis-specific Rec8 protein) as well as cohesin-
74 associated factors such as the condensins are key components of the AEs. Cohesins
75 form ring-shaped complexes that associate sister chromatids together after
76 replication and that in *S. cerevisiae* anchor the other axial element proteins to
77 chromatin (Sun et al., 2015). The HORMA domain proteins (Hop1 in *S. cerevisiae*,
78 HormaD1 and HormaD2 in mammals, ASY1/PAIR2 in plants, HIM-3, HTP-1, HTP-2,
79 and HTP-3 in *C. elegans*) also represent major components of the meiotic
80 chromosomal axes that in *C. elegans* constitute the linker between the cohesins and
81 the SC central element (Pattabiraman et al., 2017). In several organisms, including
82 *A. thaliana*, their axis association is negatively regulated by synapsis (Börner et al.,
83 2008; Wojtasz et al., 2009; Lambing et al., 2015). The last class of known axial
84 element proteins contains the *S. cerevisiae* Red1, the mouse SYCP2 and SYCP3
85 (SCP2 and SCP3 in rat), and the plant ASY3/PAIR3/DSY2 (Wang et al., 2011;
86 Ferdous et al., 2012; Lee et al., 2015). All these proteins are meiosis-specific
87 components of the axial element. Red1, SYCP2/SCP2 and ASY3/PAIR3 are large
88 proteins that show limited sequence similarities, suggesting that they could be
89 distantly related (Offenberg et al., 1998; Ferdous et al., 2012). Concerning the
90 mammalian SYCP3/SCP3, they are small proteins that show sequence similarities
91 with SYCP2/SCP2 with which they interact through their coiled-coil regions. They are
92 thought to represent key structural components of the mammalian meiotic
93 chromosome axes since notably, they form multi-stranded fibres that mimic the AEs
94 when ectopically expressed in somatic cells (Yuan et al., 1998; Pelttari et al., 2001).
95 In addition, structural resolution of the human SYCP3 protein revealed that it forms
96 elongated helical tetrameric structures that self-assemble into AE-like fibres that
97 possess the intrinsic capacity of mediating dsDNA compaction (Syrjänen et al., 2014;
98 Syrjänen et al., 2017).

99

100 Mutants defective in any component of the AE exhibit substantial perturbation of the
101 meiotic recombination process. The plant HORMA domain-containing protein ASY1
102 is not required for normal DSB formation but for DMC1 stabilisation on recombination
103 sites (Armstrong et al., 2002; Sanchez-Moran et al., 2007). In consequence, in *asy1*
104 mutants, meiotic DSBs are predominantly repaired using a sister chromatid as
105 template, as is the case in a *dmc1* mutant, provoking a shortage in CO formation

106 (Sanchez-Moran et al., 2007). The axial protein ASY3/PAIR3/DSY2, on the other
107 hand, is required for normal levels of DSB formation in *A. thaliana* and in maize
108 (Ferdous et al., 2012; Lee et al., 2015). It is also required for normal ASY1 assembly
109 onto the chromosome axis, and it interacts with ASY1 (Ferdous et al., 2012; Lee et
110 al., 2015) and with ZYP1 (Lee et al., 2015).

111

112 In this manuscript, we present the identification of ASY4, a short coiled-coil
113 containing protein showing similarity with the ASY3 C-terminus coiled coil region. We
114 show that ASY4 is an axis-associated protein that interacts with ASY1 and ASY3. We
115 also found that ASY4 is required for normal ASY1 and ASY3 localisation, for full
116 synapsis and for CO formation.

117

118

119

121 **Results**

122

123 **Identification of *ASY4*, a meiotic gene with similarity to *ASY3***

124

125 A BlastP search against the *A. thaliana* genome using the ASY3 protein (At2G46980)
126 as a query identified the uncharacterised At2g33793 protein (hereafter called ASY4)
127 as showing 29% identity and 45% similarity with 142 aa of the C-terminus region of
128 ASY3 (Figure 1). While ASY3 is a large protein (793 aa, 88 kD), ASY4 is only 212 aa
129 long (25kD). Its sequence does not contain any known functional domains and most
130 of the ASY4 protein is predicted to form coiled-coils (aa 71-183, Figure 1). ASY4
131 homologous proteins can be identified in *Tracheophyta* sequenced genomes (that
132 include flowering plant genomes and *Sellaginella moellendorffii*). Outside
133 *Tracheophyta*, ASY4 homologous sequence is found in *Marchantia polymorpha* but
134 not in mosses. RT-PCR on cDNAs isolated from different organs from wild-type
135 plants showed that *ASY4* is expressed predominantly in flower buds (SupData_1).

136

137 To analyse *ASY4* function, we characterised two independent mutant lines in
138 At2g33793. One was available in the public databases: line SK22114 (Stock:
139 CS1006148, later referred to as *asy4-1*). The second one (*asy4-2*) was isolated by
140 PCR-screening of MPIPZ (Cologne) *A. thaliana* T-DNA insertion mutants (Ríos et al.,
141 2002). Insertions in *asy4-1* and *asy4-2* are located in *ASY4* fourth and fifth exons,
142 respectively and are associated with deletions of 17 and 19 bp respectively (Figure 1
143 and SupData_2). Residual transcription corresponding to the 5' end of the gene can
144 be detected in both mutants (SupData_1). They could potentially generate a C-
145 terminally truncated protein of 92 or 106 aa respectively.

146

147 Both *asy4* mutants investigated in this study showed normal vegetative growth (not
148 shown) but fertility defects (SupData_3) that correlated with meiotic defects (Figure
149 2). During prophase I in wild-type meiosis the ten *A. thaliana* chromosomes
150 condense and recombine resulting in the formation of five bivalents, each consisting
151 of two homologous chromosomes attached to each other by sister chromatid
152 cohesion and chiasmata (the cytological manifestation of COs), which become visible
153 at diakinesis. Synapsis (the close association of two chromosomes mediated by the
154 SC) begins at zygotene and is complete by pachytene. At metaphase I, the five

Figure 1

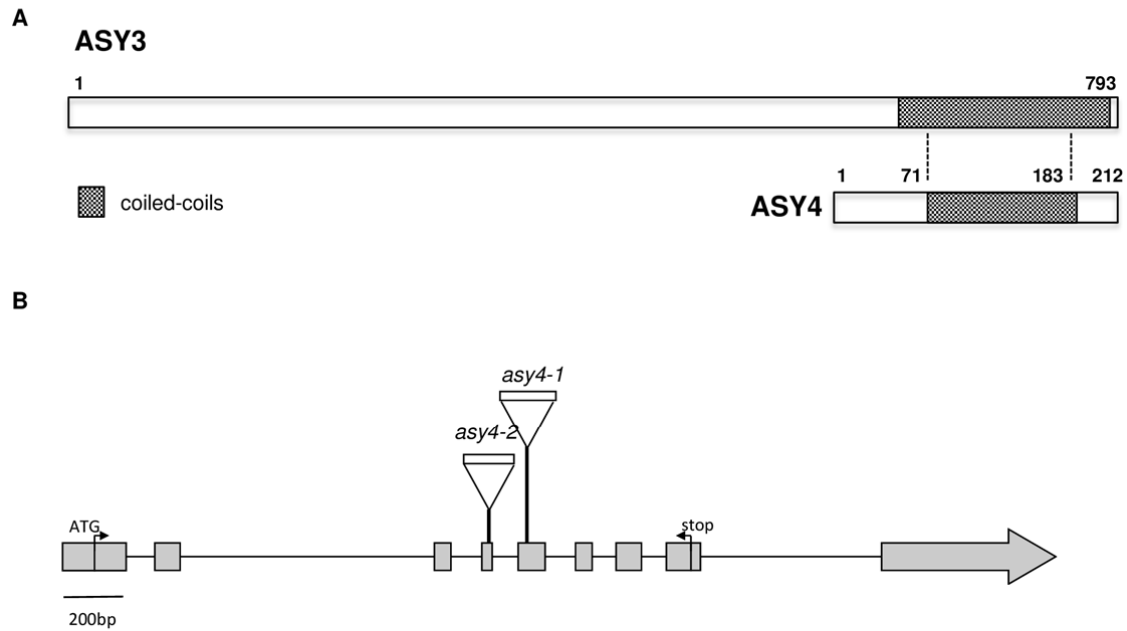


Figure 1:: Schematic representation of ASY4 protein and gene.

A. The ASY4 protein shows similarities with ASY3 C-terminal region (dashed lines).

Predicted coiled-coils of both proteins are indicated by grey boxes.

B. ASY4 open reading frame and position of the T-DNA insertion in *asy4-1* and *asy4-2* mutants. Exons are shown as grey boxes.

155 bivalents are easily distinguishable aligned on the metaphase plate. During
156 anaphase I, each chromosome separates from its homologue, leading to the
157 formation of dyads corresponding to two pools of five chromosomes. The second
158 meiotic division then separates the sister chromatids, generating four pools of five
159 chromosomes, which gives rise to tetrads of four haploid daughter cells. In *asy4*
160 mutants, each of these meiotic stages can be identified, although full synapsis was
161 not detected. Moreover, the presence of univalent chromosomes at diakinesis and
162 unbalanced tetrads (illustrated for *asy4-1* in Figure 2) indicates a defect in CO
163 formation.

164

165 The reduction in chiasma number observed in *asy4* meiocytes was quantified at the
166 transition between metaphase I and anaphase I by estimating the number of chiasma
167 based on bivalent shape. Rod bivalents reflect the occurrence of a minimum of one

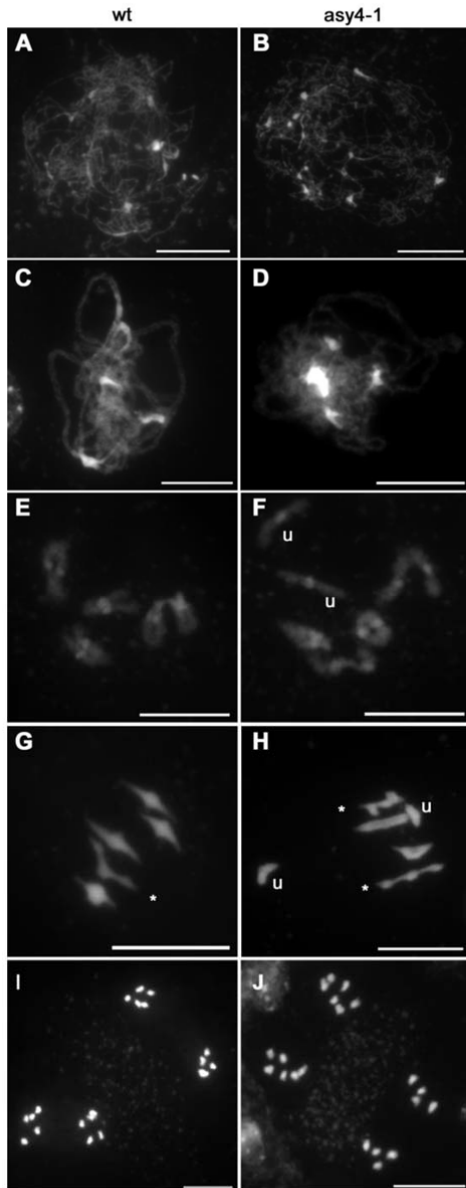
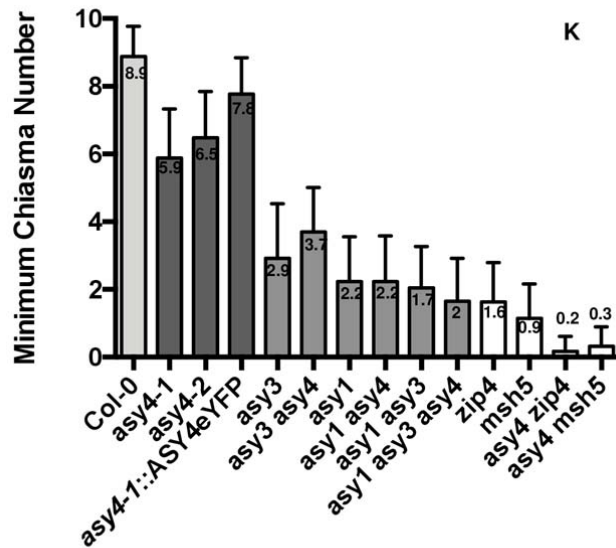


Figure 2: ASY4 is required for normal meiosis.

(A-J) DAPI staining of meiotic chromosomes in wild type (A,C,E,G,I) and *asy4-1* (B,D,F,H,J). (A,B) Leptotene; (C) Pachytene; (D) Partial synapsis typical of the defects of synapsis observed in *asy4* mutants; (E,F) Diakinesis; (G,H) Metaphase I; (I,J) End of Anaphase II. u: univalent; *: rod bivalent. Scale bars = 5 μm

(K) Quantification of the number of chiasma that can be identified at metaphase I (minimum chiasma number, MCN) in both *asy4* mutants as well as in a series of mutants and multi-mutants. Numbers give the average MCN per cell. The detailed data set can be found in SupData_4.



168 chiasma on a single chromosome arm pair whereas ring bivalents reflect the
 169 occurrence of at least one chiasma per chromosome arm. This estimation provides a
 170 minimum chiasma number (MCN, as defined in (Jahns et al., 2014)), because
 171 multiple chiasmata on a single bivalent arm cannot generally be discriminated from
 172 single chiasma. In both *asy4* mutants MCN is significantly decreased in comparison
 173 to wild type, with the *asy4-1* allele being the most affected, showing an average of
 174 5.9 ± 1.5 MCN/cell (in wild type the mean number of MCN per cell is 8.9 ± 0.89 , t test
 175 $P < 0.0001$) (Figure 2 and SupData_4). In consequence, all subsequent analyses
 176 were conducted with *asy4-1*.
 177

178 This phenotype of a decrease in chiasma formation associated with abnormal
179 synapsis has previously been described for mutants defective in axis formation
180 typified by *asy1* and *asy3* (Armstrong et al., 2002; Ferdous et al., 2012). We
181 therefore analysed the epistatic relationships between these various mutations. This
182 revealed that, in terms of chiasma level, the *asy1* mutation is epistatic to *asy3* and
183 *asy4*, with *asy1 asy3* and *asy1 asy4* double mutant combinations showing only 2
184 MCN/cell (Figure 2, and SupData_4). When analysing the double mutant *asy3 asy4*
185 however, we found that the average number of chiasmata per cell is intermediate
186 between *asy3* and *asy4* (4.1 ± 1.3 MCN/cell) and significantly different from each
187 single mutant (one-way ANOVA, $P < 0.0005$).

188

189 ***asy4* mutants are defective in meiotic recombination**

190

191 In order to understand the origin of the reduced chiasma formation observed in *asy4*,
192 we investigated meiotic recombination in further detail. First, we immunolocalised
193 DMC1, a meiosis-specific recombinase, that forms foci at recombination sites. In wild
194 type, DMC1 foci appear at late leptotene/early zygotene reaching an average of 240
195 foci per nucleus (Chelysheva et al., 2007). In *asy4-1*, we counted an average of 222
196 ± 107 ($n=15$) foci per cell suggesting that early recombination events are not affected
197 in *asy4* (SupData_5). We then immunolocalised the ZMM proteins MSH5, the MutS
198 homolog, that is involved in the stabilization of progenitor double-Holliday Junctions
199 and HEI10 which has been shown to mark a subset of recombination intermediates
200 that are channelled into the ZMM pathway (Snowden et al., 2004; Higgins et al.,
201 2008; Chelysheva et al., 2012). MSH5 foci were detected in both wild type and *asy4-1*
202 at late leptotene/early zygotene (Figure 3, A-B). No significant difference in the
203 number of foci was observed (wild type = 110.9 ± 38.61 , $n=15$; *asy4-1* = $121.1 \pm$
204 29.55 , $n=15$; Mann-Whitney U test, $P = 0.3835$). This implies that recombination in
205 *asy4-1* progresses beyond DMC1 catalysed strand-invasion. HEI10 is loaded early
206 during prophase I on a large number of recombination sites, forming foci of different
207 sizes on chromosomes. As meiosis progresses, HEI10 foci become brighter and
208 associated with the central element of the SC (ZYP1) (Figure 3C). During pachytene
209 a limited number of these foci remain at sites that correspond to class I COs where
210 they co-localise with MLH1 until the end of prophase (not shown). In *asy4-1*, the
211 HEI10 dynamics was similar as in wild type, with mixed sized foci co-localising with

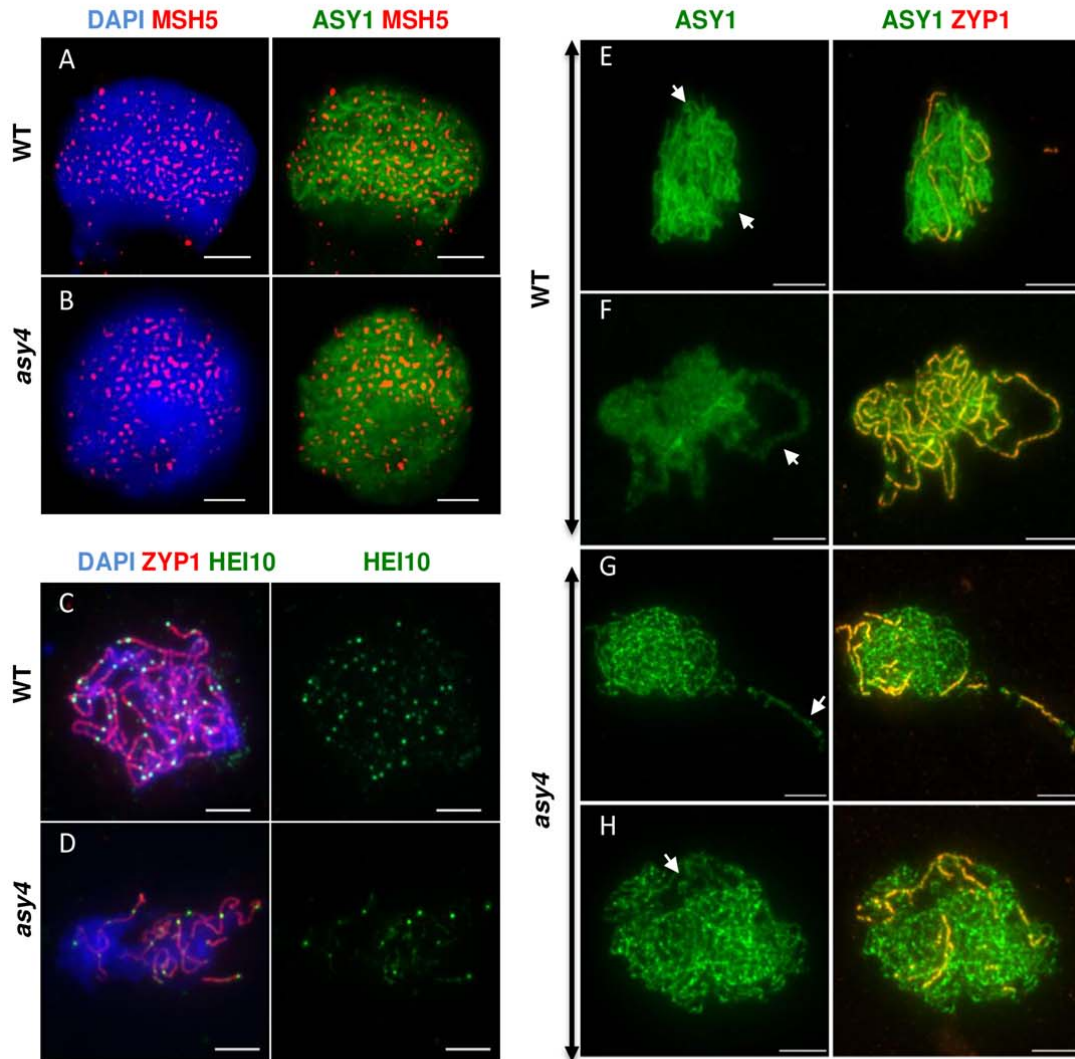


Figure 3: *asy4* mutant is defective in recombination, axis biogenesis and synapsis.

A-B: Dual ASY1 and MSH5 immuno-detection. ASY1(green), MSH5 (red), DAPI (blue). Images are a single frame from mid Z-stack. Scale bars = 2 μm

C-D: Dual ZYP1 and HEI10 immuno-detection together with DAPI (Blue) on male meiocytes at comparable stage. Scale bars = 2 μm

E-H: Dual ASY1 (green) and ZYP1 immuno-detection (red).

Arrows indicate synapsed regions where ASY1 is depleted in wild type but not in *asy4-1*. Scale bars = 2 μm

212 ZYP1 while synapsis progresses (Figure 3D). However, ZYP1 staining was very
 213 limited, never progressing to full synapsis, confirming the chromosome synapsis

214 defects detected after DAPI staining of the chromosomes (Figure 2). In
215 consequence, the pachytene-like HEI10 foci observed on the partially synapsed
216 nuclei were strongly decreased in comparison to wild type (Figure 3D).

217

218 We then analysed the level of recombination in four genetic intervals located on
219 chromosome 5 using the Fluorescent Tagged Lines (FTL) tool developed by
220 Copenhaver et al. (Berchowitz et Copenhaver, 2008). For most intervals (3 out of 4)
221 recombination rates decrease significantly but moderately in *asy4*, reaching on
222 average 75% of the wild-type level of recombination (Table 1). This effect is
223 comparable to the decrease in chiasma number observed in *asy4* (Figure 2).
224 However, the I5b interval, which is distally located on chromosome 5, appears
225 differentially affected since meiotic recombination increases slightly but significantly
226 in *asy4* (from 16 to 20 cM) (Table 1). In conclusion, *asy4* mutation provokes a
227 decrease in meiotic recombination, but this effect appears to vary according to the
228 chromosomal intervals considered.

229

230 In *A. thaliana*, most COs (85%) exhibit interference. From the FTL data, we
231 estimated the level of interference between COs in each interval by calculating the
232 ratio between the observed number of double COs to the expected number of double
233 COs under the hypothesis of no interference (NPD ratio as defined by (Snow, 1979)).
234 We observed that in most intervals considered, in *asy4* as in wild type, the NPDr is
235 smaller than 1, revealing the presence of interference between adjacent COs. Then
236 the interference between COs occurring in adjacent intervals (I5a/I5b or I5c/I5d) was
237 estimated by calculating the interference ratio (IR) as defined by Malkova et al.
238 (Malkova et al., 2004). The IR compares the genetic length of one interval with and
239 without the presence of a simultaneous event in the neighbouring interval. When the
240 occurrence of a CO in one interval reduces the probability of a CO occurring in the
241 adjacent interval, the IR is less than 1, indicating CO interference. When COs in the
242 two adjacent intervals are independent of each other, the IR is 1, and if the presence
243 of one CO in an interval increases the probability of an additional CO in the adjacent
244 interval, the IR is greater than 1, indicating negative interference. IRs revealed the
245 presence of interference between COs in wild type (for both pairs of intervals) and for
246 *asy4* for the I5c/I5d pair of intervals (Table 1). However, for the I5a/I5b pair of

247 intervals, the IR in *asy4* is above 1, suggesting that in that chromosomal region
248 adjacent COs occur more frequently than in wild type.

249

250 In wild-type *Arabidopsis*, the majority of COs (85%–90%) depend on the ZMM
251 proteins (MSH4, MSH5, MER3, ZIP4, SHOC1/ ZIP2, HEI10, and PTD) as well as on
252 MLH1 and MLH3 (Mercier et al., 2015). We analysed chiasma frequencies in *asy4*
253 *zip4* and *asy4 msh5* double mutants (Figure 2). In both cases, the level of bivalent
254 formation was dramatically reduced by more than 95%, showing that almost all the
255 COs in *asy4* are ZMM-dependent. We then estimated the average number of these
256 class I COs in *asy4* mutant by immuno-labelling chromosomes with antibodies
257 directed against MLH1, a marker of class I COs (Figure 4). We found that *asy4-1*
258 shows a limited but significant decrease in MLH1 foci from 11 ± 1.5 (mean \pm SD;
259 $n=60$) in wild type to 8.6 ± 2.2 ($n=147$) in *asy4-1* (t-test, $P<0.05$), confirming the
260 above genetic results that *asy4* mutation decreases CO formation. We then analysed
261 the distribution of these foci within bivalents. We kept in our analysis all pairs of
262 chromosome arms where at least one MLH1 foci can be observed at diakinesis. In
263 wild-type meiocytes the mean number of MLH1 foci per chromosome arm is $1.4 \pm$
264 0.52 ($n=180$) (range 1-3) whereas in *asy4-1* it increased highly significantly
265 ($P<0.0001$, t test) to a mean of 1.8 ± 0.85 ($n=134$), with a much greater range of
266 values than in wild type (1- 6 compared to 1-3 in wild-type). These cytological data
267 are in agreement with the FTL analyses and show that *asy4* mutation perturbs
268 meiotic recombination quantitatively (by decreasing it) and qualitatively (by altering
269 CO location).

270

271 ***asy4* mutation is associated with axis defects**

272

273 We investigated the behaviour of several components of the meiotic chromosome
274 axis (ASY1, ASY3, REC8 and SCC3) in the *asy4* mutant in comparison to wild type
275 (Figure 3, Figure 5, and SupData_6). ASY1, ASY3, REC8 and SCC3 are detected
276 during meiotic prophase I and exhibit different dynamics as meiosis progresses
277 (Armstrong et al., 2002; Cai et al., 2003; Chelysheva et al., 2005; Ferdous et al.,
278 2012). At leptotene, all these proteins brightly decorate meiotic chromosomes,
279 revealing the typical thread-like chromosomal axis. As synapsis proceeds and the
280 central element connects the axial elements of the homologous chromosomes, ASY1

Figure 4

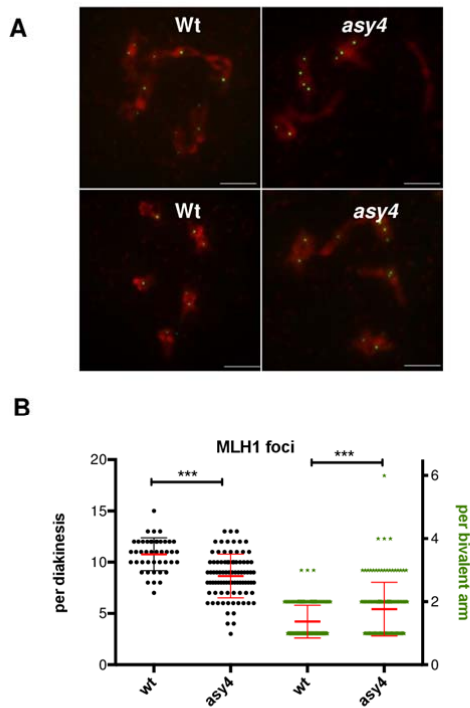


Figure 4 : MLH1 detection and quantification.

(A) MLH1 was immunolocalised (green) on diakinesis chromosomes from wild-type (wt) or *asy4-1* (*asy4*) mutant. Chromosomes were stained by DAPI (red). Scale bars = 5 μ m

(B) Average number of MLH1 foci per cell (black) or per bivalent arm (green).

281 is depleted from the axis and consequently the ASY1 signal appears faint and fuzzy
282 (Figure 3 arrows, SupData_6). ASY3, REC8 and SCC3 also mark the chromosome
283 axes, but contrary to ASY1, they are not removed during synapsis (Figure 5 and
284 SupData_6). In the case of the cohesins REC8 and SCC3, no obvious modification in
285 their pattern could be detected (Figure 5 and SupData_6). The two axis-associated

286 proteins ASY1 and ASY3 are loaded onto the chromosome axis and chromosome
287 threads typical of leptotene stages can be seen. However, ASY1 and ASY3 signals
288 adopt an abnormally patchy and lumpy aspect (Figure 3 and Figure 5), suggesting
289 that in *asy4*, the meiotic chromosome axis is aberrantly structured. In addition, we
290 observed no displacement of ASY1 from the synapsed chromosome axes (Figure 3),

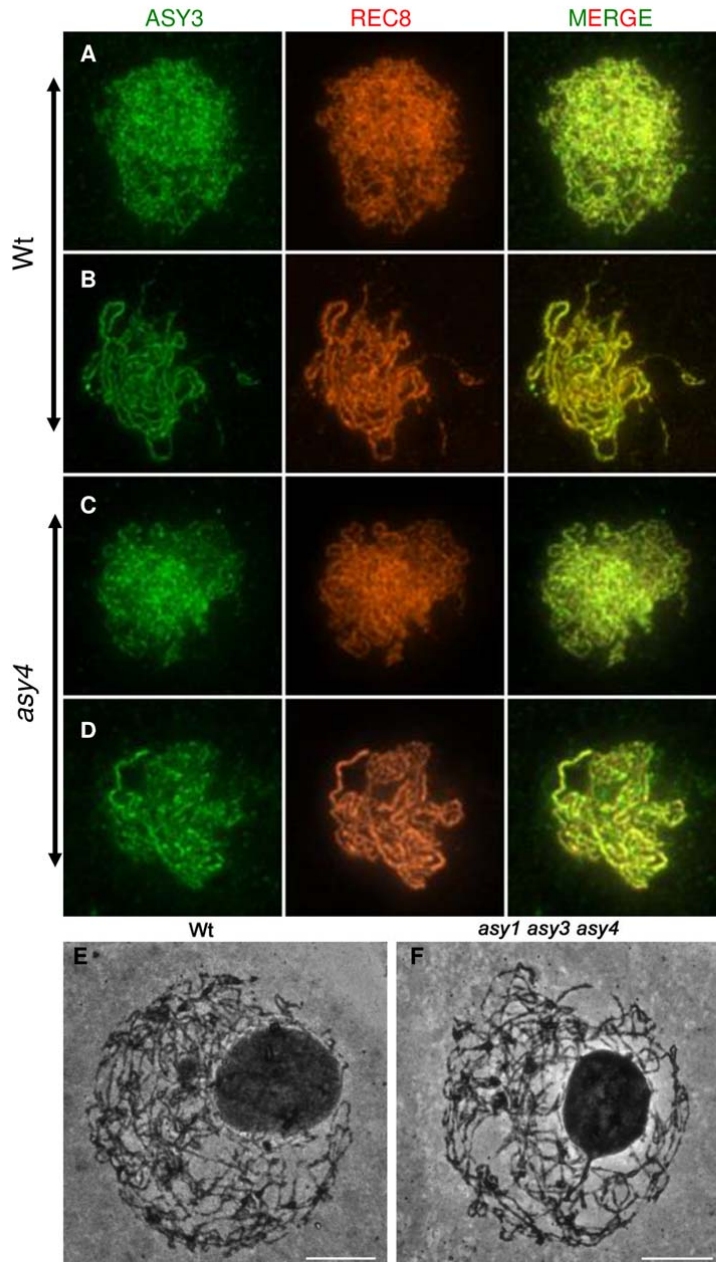


Figure 5 : Chromosome axis investigation

(A-D) Dual ASY3 (green) and REC8 (orange) immunolocalisation on wild-type (A,B) or *asy4-1* mutant (*asy4*) (C,D) male meiocytes. (E,F) Silver staining of wild-type (wt) and triple *asy1asy3asy4* mutant male meiocytes. Scale bars = 2 μ m

291 revealing abnormal axis dynamics. We investigated the chromosome axis further by
 292 silver-staining of chromosome spreads and wide-field microscopy observation as
 293 described in (Armstrong and Jones, 2001). This chromatin staining permits the
 294 detection of the meiotic chromosome axis from leptotene to the end of meiosis. In the
 295 *asy4* mutant but also in *asy3 asy4* and *asy1 asy3 asy4*, no modification of the silver-

296 stained axis could be detected (Figure 5), suggesting that even if axis composition
297 and/or dynamics is affected in *asy4*, at this level of resolution the overall structure of
298 the axis appears physically intact.

299

300 **ASY4 is an axial-associated protein**

301

302 To examine the cellular localisation of ASY4 we used fluorescent protein tagging. An
303 ASY4-eYFP construct was produced and introduced into homozygous *asy4-1* plants,
304 the most severely affected mutant background. Seed counts were performed on
305 siliques from T2 generation plants (SupData_7). Fertility levels across the
306 transformant lines were wide ranging, from those comparable to *asy4-1*, to a line that
307 was not significantly different to wild-type (line 165.15, subsequently referred to as
308 *asy4-1::ASY4eYFP*; SupData_7). Analysis of DAPI-stained chromosome spreads of
309 *asy4-1::ASY4eYFP* male meiocytes from T3 plants at metaphase I revealed a
310 chiasma frequency of 7.7 ± 1.1 (n=75). This was significantly higher than *asy4.1* (5.9
311 ± 1.43 (n= 64); Mann-Whitney U test, $p < 0.01$). However, it was slightly lower than
312 wild-type (8.6 ± 0.83 (n=28); (Mann-Whitney U test, $p < 0.01$)) (Figure 2, SupData_7).
313 In addition, occasional seed gaps in its siliques were apparent, suggesting that
314 fertility was not completely restored (SupData_7).

315

316 Examination of the anthers from *asy4-1::ASY4eYFP* using epi-fluorescence
317 microscopy confirmed expression of the tagged gene within male meiocytes
318 (SupData_7). Localization of ASY4eYFP was then investigated in prophase I
319 chromosome spread preparations by direct fluorescence combined with immuno-
320 staining of the chromosome axis protein, ASY1 and the SC protein, ZYP1. This
321 revealed that ASY4 localises as a linear, axis-associated signal at leptotene where it
322 follows the localisation pattern of ASY1 with alternating regions of high and low
323 intensity (Figure 6). However, in contrast to ASY1 which becomes depleted from the
324 axes as zygotene progresses, it persists on synapsed regions of the chromosomes
325 (Figure 6). In this respect, its behaviour is similar to that of ASY3, REC8 and SCC3.

326

327 Considering the similarity between the ASY3 and ASY4 protein sequences, the axial
328 association of these two proteins ((Ferdous et al., 2012) and this study), and the
329 perturbed ASY1 and ASY3 signals observed in *asy4*, we investigated whether these

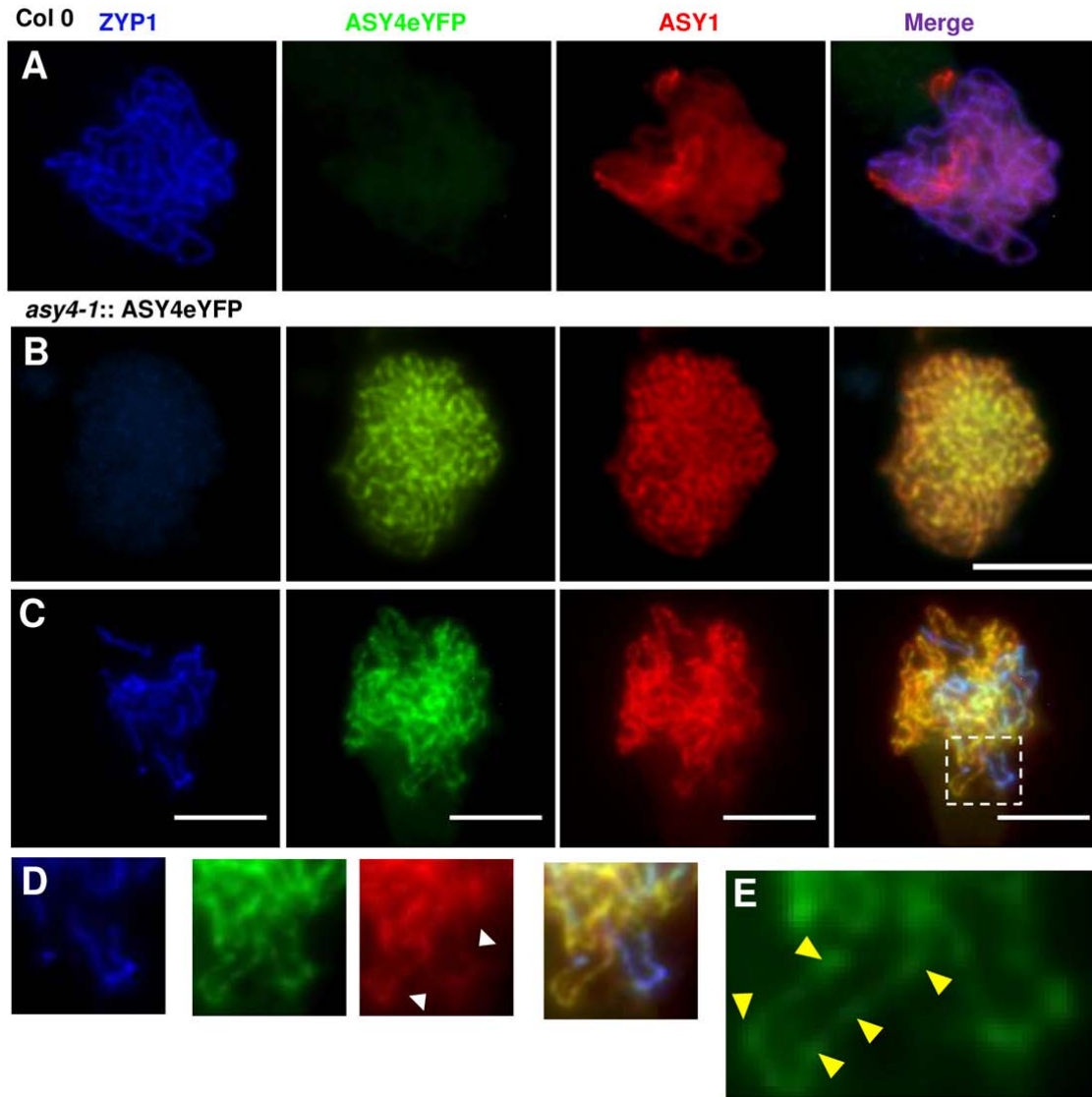


Figure 6: Localization of ASY4eYFP in prophase I chromosome spreads of *asy4-1::ASY4eYFP*. (A) Wild-type (Col 0) zygote showing absence of eYFP fluorescence. (B) *asy4-1::ASY4eYFP* leptotene and (C) *asy4-1::ASY4eYFP* zygotene. (D) Detail shows the ASY4eYFP fluorescence present on the axis in regions of intense ASY1 staining (unsynapsed) and ZYP1 staining (synapsed). Note reduction in intensity of ASY1 signal in synapsed regions (white arrows). (E) ASY4eYFP fluorescence is not uniform and alternates between regions of high (arrowed) and low intensity. ZYP1 (blue), and ASY1 (red) immunostaining with ASY4-eYFP fluorescence (green). Scale bars = 5 μ m

330 proteins physically interact. Interaction between ASY1 and ASY3 has already been
 331 demonstrated for *Brassica oleracea* and *Arabidopsis* proteins either *in planta* by co-
 332 immunoprecipitation of ASY3 from anthers by antibodies directed against ASY1 or in
 333 yeast two hybrid (Y2H) experiments using the *A. thaliana* proteins (Ferdous et al.,

Figure 7

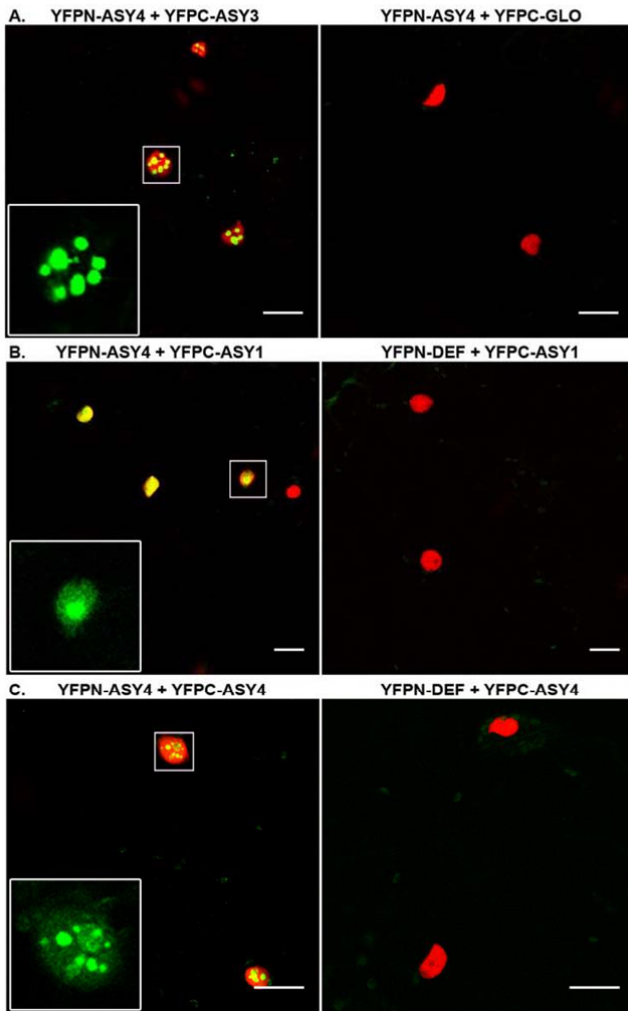


Figure 7: Split-YFP assays in *N. benthamiana* epidermal cells.

N. benthamiana epidermal cells were co-infiltrated with *Agrobacterium* cultures expressing two complementary YFP fusions (N or C-terminal truncations, YFPN or YFPC). Nuclei are identified thanks to a constitutively-expressed fluorescent nuclear protein (H2B-CFP, here shown in red). Interaction between the two tested proteins revealed a YFP signal (green). For each interaction tested, a negative control corresponding to the co-infiltration of one of the fusion protein of interest with the complementary YFP moiety fused with an unrelated protein (*Anthirrinum majus* MADS box transcription factors DEFICIENS -DEF- or GLOBOSA -GLO-). The complete set of split-YFP data can be found in SupData_8. Scale bars = 25 μ m

334 2012). Here, we used bimolecular fluorescence complementation assays in leaf
335 epidermal cells of *Nicotiana benthamiana* plants (BiFC) (Hu et al., 2002). Fusion
336 proteins with complementary YFP truncations (YFP^N + YFP^C) were co-infiltrated in *N.*
337 *benthamiana* leaves expressing a CFP nuclear marker. As shown in Figure 7 and

338 SupData_8, this assay revealed interactions among the three ASY proteins and also
339 self-interaction of these three proteins. The YFP signal recovered in these
340 experiments using ASY3 or ASY4 fusion proteins revealed non-uniform nucleus-
341 targeted signals, suggesting that these proteins when overexpressed in plant cells
342 form nuclear aggregates. Y2H experiments confirmed ASY3/ASY4 interactions as
343 well as ASY3/ASY3 and ASY4/ASY4 self-interactions (SupData_9).
344

346 **Discussion**

347

348 **Identification of a new component of the meiotic chromosome axis**

349 We identified the ASY4 protein that shows sequence similarity with the ASY3 C-
350 terminal region and that is closely related with two of the known plant axial
351 components, ASY1/PAIR2 and ASY3/PAIR3/DSY2. The three proteins interact
352 together and ASY4 is required for normal loading and/or stabilisation of ASY1 and
353 ASY3 onto chromosomes. We also found that an ASY4-eYFP fusion protein is axis-
354 associated, leading us to conclude that ASY4 is a new component of the meiotic
355 chromosome axis.

356 The link between ASY3 and ASY4 can be viewed as a parallel with those existing
357 between the mammalian SYCP2/SCP2 and SYCP3/SCP3: ASY3 and SYCP2/SCP2
358 are large proteins that show limited sequence similarities with the small coiled-coil
359 proteins ASY4 and SYCP3/SCP3 respectively (as an example SCP3 shows 19% aa
360 identity and 47% aa similarity with the last 163 aa of SCP2); ASY3 and ASY4 interact
361 together (this study) as well as the mammalian SYCP3 and SYCP2 (Yang et al.,
362 2006); all these proteins are axial associated proteins (Offenberg et al., 1998; Schalk
363 et al., 1998; Yang et al., 2006; Ferdous et al., 2012) (this study). In addition, limited
364 sequence similarities can be detected between ASY3/SYCP2 and the *S. cerevisiae*
365 Red1 axial component (Offenberg et al., 1998; Ferdous et al., 2012). The close
366 interconnection between these proteins and the HORMA domain-containing proteins
367 ASY1 in plants (this study and (Wang et al., 2011; Ferdous et al., 2012; Lee et al.,
368 2015)) and HormaD1 and D2 in mammals (Wojtasz et al., 2009) suggests that all
369 together they form a protein complex crucial for the biogenesis of the meiotic
370 chromosome axis scaffold. Taken together these data suggest that ASY3/ASY4 are
371 the functional homologues of the mammalian SYCP2/SYCP3. It is interesting to note
372 that these proteins of the AE as well as those that form the CE of the SC are very
373 poorly conserved at the sequence level but all show the same structure and
374 assembly characteristics (Fraune et al., 2016). This limited sequence conservation
375 among SC proteins from different species is probably due to rapid sequence
376 divergence as has been observed for plant and mammalian SC proteins (Ferdous et
377 al., 2012; Fraune et al., 2016).

378

379 **ASY4 is required for normal meiotic recombination**

380 According to chiasma and MLH1 counting and to genetic measurement of
381 recombination using FTL lines, CO formation is reduced by a factor of 1.5 in *asy4*
382 mutants. This was correlated with a clear decrease in HEI10 and MLH1 foci at late
383 prophase I and diakinesis, showing that ASY4 is required for normal recombination. It
384 should be noted that the CO decrease observed in *asy4* is lower than the one
385 associated with disruption of either of the two ASY4 partners, ASY1 and ASY3. In
386 terms of chiasma level, the *asy1* mutation is the most affected and is epistatic to *asy3*
387 and *asy4*. This suggests that among the three axis components ASY1, ASY3 and
388 ASY4, the HORMA-domain containing protein ASY1 is a key player, while ASY3 and
389 ASY4 could be seen as accessory proteins. Nevertheless, we cannot exclude the
390 possibility that the partially penetrant phenotype of *asy4* is due to leaky mutations
391 since we could detect the transcription of the 5' end of the gene in both mutants.

392 Interestingly we observed that the decrease in recombination observed in *asy4*
393 mutants is differentially distributed within the genome since we found that one
394 interval out of four tested (I5b) revealed an increase in CO level (from 16 to 20 cM).
395 This could be related to the distal location of this interval on chromosome 5 and to
396 the observation that the vast majority of chiasma are terminally-located in *asy3* and
397 *asy1* mutants (Ross et al., 1997; Ferdous et al., 2012). Two other findings of our
398 study confirm that CO location is modified in *asy4*. First, despite the average
399 decrease in MLH1 foci in *asy4* mutants, we detected an increased number of MLH1
400 foci per chromosome arm in comparison to wild type, with up to 6 foci in the same
401 arm while we have never observed more than 3 per chromosome arm in wild type.
402 Second, we found an interference ratio greater than 1 for one pair of intervals tested
403 by FTL (I5a/I5b). This latter result involves the I5b terminally located interval on
404 chromosome 5, suggesting that the two phenomena may be connected and that, in
405 *asy4*, COs are not only decreased but also tend to group in the distal parts of the
406 chromosomes. In this regard, it is interesting to note that we reported recently that, in
407 *Arabidopsis* as in most species, synapsis is preferentially initiated from the distal
408 parts of the chromosomes (Hurel et al. Plant J. in press). If this is also the case in
409 *asy4*, the limited number of ZYP1-labelled central elements on which recombination
410 events appear to be restricted (according to HEI10 labelling, Figure 3) are expected
411 to be predominantly distally located. This could explain why we observed a bias in
412 location of the COs in *asy4*. Further studies will be required to confirm these
413 observations genome-wide and to understand the mechanisms involved.

414 According to our study, the decrease in CO formation measured in *asy4* is not
415 correlated with a decrease in the overall number of early initiation events since the
416 number of DMC1 and MSH5 foci was unchanged in *asy4-1* in comparison to wild
417 type. It is interesting to note that the role in recombination of the three ASY proteins
418 can be differentiated: ASY1, like ASY4, is not required for normal DSB formation but,
419 contrary to ASY4, is mandatory for the formation of stable DMC1 nucleofilaments
420 (Sanchez-Moran et al., 2007) while ASY3 is required at the step of DSB formation
421 (Ferdous et al., 2012). Chromosome fragmentation was not detected in *asy4*,
422 showing that the DMC1-labelled recombination events are eventually repaired, either
423 using the sister chromatid or the homologous chromosome as a template. Since the
424 number of MSH5 foci at early/mid prophase I appeared normal in *asy4-1*, it would
425 seem likely that recombination proceeds beyond the initial strand invasion stage.
426 This would imply that CO designation, which occurs in early prophase I (Lambing et
427 al., 2017), is normal in the mutant but that a proportion of the designated
428 intermediates fail to mature into COs, consistent with the observed reduction in
429 MLH1 and HEI10 foci. The defect in SC polymerization observed in *asy4* may result
430 in CO designated recombination intermediates that lie within regions of the homologs
431 that remain aysynaptic failing to form COs. Establishing the exact relationship
432 between the loss of ASY4 and the defect in SC formation will be the target of future
433 investigation.

434

435

436

437

438

439 **Materials and Methods**

440

441 **Plant material and growth conditions**

442 *asy4-1* (SK22114, CS1006148) was available in the public databases and was
443 provided by the NASC (<http://arabidopsis.info/>) (Scholl et al., 2000). *asy4-2* (line
444 65433) was identified through a PCR-based screen of the Koncz's collection (Ríos et
445 al., 2002). Other mutant alleles used in this study are *asy1* (SALK_046272,
446 N546272), *asy3* (SALK_143676, N643676), *dmc1* (SAIL_170_F08, N871769), *mer3*
447 (SALK_091560, N591560), *mlh1* (SK25975, N1008089), *msh5* (SALK_026553,
448 N526553), *rad51* (GABI_134A01) and *zip4* (SALK_068052, N568052). Genotyping
449 conditions and primer sequences are given in SupData_10 and SupData_11).

450

451 *Arabidopsis thaliana* and *Nicotiana benthamiana* plants were grown in the
452 greenhouse (photoperiod 16 h/day and 8 h/night; temperature 20°C day and night;
453 humidity 70%; photoperiod 13 h/day and 11 h/night; temperature 25°C day and 17°C
454 night, respectively).

455

456 **Clone construction**

457 ASY4 cDNA was amplified on flower bud cDNA (Col-0) after two rounds of nested
458 PCR (PCR I: AtASY4RTF and AtASY4RTR, PCR II: AtASY4attB1 and AtASY4attB2,
459 SupData_10) and cloned into pDONR207 (Invitrogen) following the manufacturer's
460 instructions. The generated entry vector was sequenced and used to transfer ASY4
461 cDNA into the yeast two hybrid expression vectors pDEST-GADT7 and pDEST-
462 GBKT7 (Rossignol et al., 2007). To generate the C-terminus Split-YFP
463 clones (Azimzadeh et al., 2008), a version of the cDNA without a STOP codon was
464 amplified beforehand using primers AtASY4attB1 and AtASY4-attB2wostop
465 (SupData_10). Similar approaches were undertaken for ASY1 and ASY3 cDNAs
466 except that using primers AtASY1-attB1, AtASY3-attB1, AtASY3-attB2, AtASY3-
467 attB2wostop, and AtASY1-attB2 (SupData_10).

468

469 **Yeast two hybrid**

470 Yeast two hybrid assays were carried out using the GAL4-based system (Clontech).
471 SV40 Antigen T (AgT) and p53 protein were used as positive controls. Yeast

472 plasmids were introduced in AH109 or Y187 strains by lithium acetate transformation
473 following the protocol in the MATCHMAKER GAL4 Two hybrid System 3 manual
474 (Clontech). After mating in appropriate pairwise combinations, the resulting diploids
475 cells were selected on SD medium lacking a combination of amino acids, driven by
476 the auxotrophy genes carried by the cloning vectors. Protein interactions were
477 assayed by growing diploid cells on SD-LWH, and SD-LWHA.

478

479 **Bimolecular fluorescence complementation**

480 Protein interactions were tested *in planta* using bimolecular fluorescence
481 complementation (BiFC) assays (Hu et al., 2002) in leaf epidermal cells of *N.*
482 *benthamiana* plants expressing a nuclear cyan fluorescent protein (CFP fused to
483 histone 2B) (Martin et al., 2009). For each protein, four expression vectors were
484 produced, generating inactive N- or C-termini of the YFP (YFP^N, YFP^C) fused with the
485 target sequence in N- or C-termini. Combinations bringing together the two YFP
486 complementary regions (YFP^N + YFP^C) were co-infiltrated in *N. benthamiana* leaves
487 as described in (Azimzadeh et al., 2008; Vrielynck et al., 2016).

488

489 **Bioinformatics**

490 PSI BLAST on nr database using ASY3 as a query picked up at the first round of
491 iteration At2g33793 with its C terminal region (aa 636-777, where coiled coils lie (aa
492 625-785, according to (Ferdous et al., 2012)). BLASTP and TBLASTN on plant
493 sequenced genomes present in phytozome 12 database (Blosum45) were done to
494 identify for homologues.

495

496 **Recombination measurement**

497 We used the fluorescent-tagged lines (FTLs) described in (Berchowitz and
498 Copenhaver, 2008) to estimate recombination rates in four different genomic
499 intervals (I5a, I5b, I5c and I5d). We generated plants that were homozygous for the
500 *qrt* mutation, heterozygous for pairs of linked fluorescent markers RY/++ (I5a and
501 i5d) or YC/++ (I5b and I5c) (R red, Y yellow, C Cyan) and either wild type or
502 homozygous for the *asy4-1* mutation. Tetrad analyses were carried out as described
503 in (Berchowitz and Copenhaver, 2008) on tetrads where each fluorescent marker
504 segregated correctly.

505

506 **Fluorescent protein tagging**

507 The ASY4 genomic locus, comprising 1835 base pairs upstream of the start codon to
508 502 base pairs downstream of the stop codon and including all introns and UTRs,
509 was amplified with the primers At2g33793-P9 and At2g33793-P10 (SupData_10).
510 The eYFP sequence was inserted in frame at amino-acid position 202, downstream
511 of the predicted coiled-coil region and close to the C-terminus. The construct was
512 inserted into p35-Nos-BM cloning vector using *Sfi* I sites incorporated into the
513 primers. The resulting expression cassette was subcloned via *Sfi* I into pLH9000
514 binary vector and used for Agrobacterium-mediated transformation of plants using
515 floral dip. Transformants were selected on kanamycin (50 µg/ml) Murashige and
516 Skoog media (Murashige and Skoog, 1962).

517

518 **Cytological procedures**

519 Meiotic chromosome spreads were DAPI stained as described previously in (Ross et
520 al., 1996) or silver nitrate stained as described in (Armstrong et al., 2001).
521 Immunostaining of male meiotic spreads was carried out as in (Armstrong and
522 Osman, 2013; Chelysheva et al., 2013). Antibodies used for immunolocalisation were
523 anti-ASY1 (rat, 1 in 1000 dilution) (Armstrong et al, 2002), anti-AtZYP1 (rabbit, N-
524 terminus Ab aa residues 1-415, 1 in 500 dilution) (Higgins et al., 2005), anti-ASY3
525 (rabbit, 1 in 250 dilution) (Ferdous et al., 2012), anti-REC8 (rat, 1 in 250 dilution)
526 (Cromer et al., 2013), anti-DMC1 (rat, 1 in 20 dilution) (Vignard et al., 2007), anti-
527 MSH5 (rabbit, 1 in 200 dilution) (Higgins et al., 2008), anti-MLH1 (rabbit, 1 in 200
528 dilution) (Chelysheva et al., 2013) and anti-HEI10 (rabbit, 1 in 250 dilution)
529 (Chelysheva et al., 2012).

530

531 **Image analysis**

532 *asy4-1::ASY4eYFP* zygotene male meiocyte nucleus image was captured with Nikon
533 90i, 100x objective as a Z-stack. The green channel (eYFP) was processed as an
534 average intensity projection using Fiji, due to more rapid bleaching of eYFP relative
535 to the red (Texas red-ASY1) and blue (Alexa350-ZYP1) channels, which were
536 processed as maximum intensity projections. Col-0 was imaged using the same
537 exposure times and processed in the same way. MSH5 foci were scored using Z-
538 stack images and 'Mexican Hat' deconvolution as described in (Ferdous et al., 2012).

539

540 **Acknowledgements:**

541 We wish to thank Christine Mézard for critical reading of the manuscript. The IJPB
542 benefits from the support of the LabEx Saclay Plant Sciences-SPS (ANR-10-LABX-
543 0040-SPS). We also thank Csaba Koncz and Sabine Schäfer for giving access to the
544 MPIPZ T-DNA insertion mutant collection.

545

546 **One-sentence summary:**

547 A new component of the meiotic chromosome axis is required for normal meiotic
548 recombination and synapsis in *Arabidopsis thaliana*.

549

550 **Authors' contributions:** A.C., A.D., K.O. and A.W. performed most of the
551 experiments; D.V., C.H., L.C., A.R. and S.H. provided technical assistance, A.D.M.,
552 F.C.H.F. and M.G. conceived the experiments, F.C.H.F. and M.G. supervised the
553 writing.

554

555 **Funding information:**

556 F.C.H.F. laboratory: BBSRC grant numbers ERA-Caps-13 BB/M004902/1 and
557 MIBTP GBGB.GAM2526.

558

559 **Present addresses:**

560 S.H.: Leibniz Institute of Plant Genetics and Crop Plant Research (IPK), Stadt
561 Seeland, Germany.

562 A.D.M.: Institut Curie, PSL Research University, CNRS, UMR3664, F-75005, Paris,
563 France.

564 A.W.: Central European Institute of Technology, Masaryk University, Kamenice,
565 753/5, 62500, Czech Republic.

566 A.R.: Instituto de Biotecnología / UNAM, Av. Universidad #2001, Col. Chamilpa C.P.
567 62210, Cuernavaca, Morelos, MEXICO.

568

569 **Corresponding author email:** mathilde.grelon@inra.fr

570

571

572 **Tables**

573

574 Table 1:

575

	interval	Nb of tetrads	d (cM)	d ratio (asy4/wt)	NPD ratio	IR
wt	i5a	10,303	27	-	0.3**	0.4**
	i5b	10,303	16.1	-	0.2**	
	i5c	14,590	7.7	-	0.3**	0.3**
	i5d	14,590	7.4	-	0.3**	
asy4-1	i5a	7,462	15.5	0.6	0.9	1.2**
	i5b	7,462	20	1.2	0.6**	
	i5c	13,753	6.8	0.9	0.4**	0.7**
	i5d	13,753	5.6	0.8	0.5*	

576

577

578

579

580 **Figure Legends:**

581

582 **Figure 1: Schematic representation of ASY4 protein and gene.**

583 A. The ASY4 protein shows similarities with ASY3 C-terminal region (dashed lines).

584 Predicted coiled-coils of both proteins are indicated by grey boxes.

585 B. ASY4 open reading frame and position of the T-DNA insertion in *asy4-1* and *asy4-*

586 2 mutants. Exons are shown as grey boxes.

587

588 **Figure 2: ASY4 is required for normal meiosis.**

589 (A-J) DAPI staining of meiotic chromosomes in wild type (A,C,E,G,I) and *asy4-1*

590 (B,D,F,H,J). (A,B) Leptotene; (C) Pachytene; (D) Partial synapsis typical of the

591 defects of synapsis observed in *asy4* mutants; (E,F) Diakinesis; (G,H) Metaphase I;

592 (I,J) End of Anaphase II. u: univalent; *rod bivalent. Scale bars = 5 μ m

593 (K) Quantification of the number of chiasma that can be identified at metaphase I

594 (minimum chiasma number, MCN) in both *asy4* mutants as well as in a series of

595 mutants and multi-mutants. Numbers give the average MCN per cell. The detailed

596 data set can be found in SupData_4.

597

598 **Figure 3: *asy4* mutant is defective in recombination, axis biogenesis and**

599 **synapsis.**

600 A-B: Dual ASY1 and MSH5 immuno-detection. ASY1(green), MSH5 (red), DAPI
601 (blue). Images are a single frame from mid Z-stack. Scale bars = 2 μ m

602 C-D: Dual ZYP1 and HEI10 immuno-detection together with DAPI (Blue) on male
603 meiocytes at comparable stage. Scale bars = 2 μ m

604 E-H: Dual ASY1 (green) and ZYP1 immuno-detection (red). Arrows indicate
605 synapsed regions where ASY1 is depleted in wild type but not in *asy4-1*. Scale bars

606 = 2 μ m

607

608 **Figure 4: MLH1 detection and quantification.**

609 (A) MLH1 was immunolocalised (green) on diakinesis chromosomes from wild-type
610 (wt) or *asy4-1* (*asy4*) mutant. Chromosomes were stained by DAPI (red). Scale bars

611 = 5 μ m

612 (B) Average number of MLH1 foci per cell (black) or per bivalent arm (green).

613

614

615 **Figure 5: Chromosome axis investigation**

616 (A-D) Dual ASY3 (green) and REC8 (orange) immunolocalisation on wild-type (A,B)
617 or *asy4-1* mutant (*asy4*) (C,D) male meiocytes. (E,F) Silver staining of wild-type (wt)
618 and triple *asy1asy3asy4* mutant male meiocytes. Scale bars = 2 μ m

619

620 **Figure 6:** Localization of ASY4eYFP in prophase I chromosome spreads of *asy4-*
621 *1::ASY4eYFP*. (A) Wild-type (Col 0) zygotene showing absence of eYFP
622 fluorescence. (B) *asy4-1::ASY4eYFP* leptotene and (C) *asy4-1::ASY4eYFP*
623 zygotene. (D) Detail shows the ASY4eYFP fluorescence present on the axis in
624 regions of intense ASY1 staining (unsynapsed) and ZYP1 staining (synapsed). Note
625 reduction in intensity of ASY1 signal in synapsed regions (white arrows). (E)
626 ASY4eYFP fluorescence is not uniform and alternates between regions of high
627 (arrowed) and low intensity. ZYP1 (blue), and ASY1 (red) immunostaining with
628 ASY4-eYFP fluorescence (green). Scale bars = 5 μ m

629

630

631 **Figure 7: Split-YFP assays in *N. benthamiana* epidermal cells.**

632 *N. benthamiana* epidermal cells were co-infiltrated with *Agrobacterium* cultures
633 expressing two complementary YFP fusions (N or C-terminal truncations, YFPN or
634 YFPC). Nuclei are identified thanks to a constitutively-expressed fluorescent nuclear
635 protein (H2B-CFP, here shown in red). Interaction between the two tested proteins
636 revealed a YFP signal (green). For each interaction tested, a negative control
637 corresponding to the co-infiltration of one of the fusion protein of interest with the
638 complementary YFP moiety fused with an unrelated protein (*Anthirrinum majus*
639 MADS box transcription factors DEFICIENS -DEF- or GLOBOSA -GLO-). The
640 complete set of split-YFP data can be found in SupData_8. Scale bars = 25 μ m

641

Parsed Citations

Armstrong SJ, Caryl AP, Jones GH, Franklin FCH (2002) *Asy1*, a protein required for meiotic chromosome synapsis, localizes to axis-associated chromatin in *Arabidopsis* and *Brassica*. *J Cell Sci* 115: 3645-55

Pubmed: [Author and Title](#)

CrossRef: [Author and Title](#)

Google Scholar: [Author Only](#) [Title Only](#) [Author and Title](#)

Armstrong SJ, Franklin FCH, Jones GH (2001) Nucleolus-associated telomere clustering and pairing precede meiotic chromosome synapsis in *Arabidopsis thaliana*. *J Cell Sci* 114: 4207-17

Pubmed: [Author and Title](#)

CrossRef: [Author and Title](#)

Google Scholar: [Author Only](#) [Title Only](#) [Author and Title](#)

Armstrong SJ, Jones GH (2001) Female meiosis in wild-type *Arabidopsis thaliana* and in two meiotic mutants. *Sex Plant Reprod* 13: 177-183

Pubmed: [Author and Title](#)

CrossRef: [Author and Title](#)

Google Scholar: [Author Only](#) [Title Only](#) [Author and Title](#)

Armstrong SJ, Osman K (2013) Immunolocalization of meiotic proteins in *Arabidopsis thaliana*: method 2. *Methods Mol Biol* 990: 103-7

Pubmed: [Author and Title](#)

CrossRef: [Author and Title](#)

Google Scholar: [Author Only](#) [Title Only](#) [Author and Title](#)

Azizzadeh J, Nacry P, Christodoulidou A, Drevensek S, Camilleri C, Amieur N, Parcy F, Pastuglia M, Bouchez D (2008) *Arabidopsis* TONNEAU1 proteins are essential for preprophase band formation and interact with centrin. *Plant Cell* 20: 2146-59

Pubmed: [Author and Title](#)

CrossRef: [Author and Title](#)

Google Scholar: [Author Only](#) [Title Only](#) [Author and Title](#)

Berchowitz LE, Copenhaver GP (2008) Fluorescent *Arabidopsis* tetrads: a visual assay for quickly developing large crossover and crossover interference data sets. *Nat Protoc* 3: 41-50

Pubmed: [Author and Title](#)

CrossRef: [Author and Title](#)

Google Scholar: [Author Only](#) [Title Only](#) [Author and Title](#)

Blat Y, Protacio RU, Hunter N, Kleckner N (2002) Physical and functional interactions among basic chromosome organizational features govern early steps of meiotic chiasma formation. *Cell* 111: 791-802

Pubmed: [Author and Title](#)

CrossRef: [Author and Title](#)

Google Scholar: [Author Only](#) [Title Only](#) [Author and Title](#)

Börner GV, Barot A, Kleckner N (2008) Yeast Pch2 promotes domainal axis organization, timely recombination progression, and arrest of defective recombinosomes during meiosis. *Proc Natl Acad Sci U S A* 105: 3327-32

Pubmed: [Author and Title](#)

CrossRef: [Author and Title](#)

Google Scholar: [Author Only](#) [Title Only](#) [Author and Title](#)

Cai X, Dong F, Edelmann RE, Makaroff CA (2003) The *Arabidopsis* SYN1 cohesin protein is required for sister chromatid arm cohesion and homologous chromosome pairing. *J Cell Sci* 116: 2999-3007

Pubmed: [Author and Title](#)

CrossRef: [Author and Title](#)

Google Scholar: [Author Only](#) [Title Only](#) [Author and Title](#)

Chelysheva LA, Grandont L, Grelon M (2013) Immunolocalization of meiotic proteins in Brassicaceae: method 1. *Methods Mol Biol* 990: 93-101

Pubmed: [Author and Title](#)

CrossRef: [Author and Title](#)

Google Scholar: [Author Only](#) [Title Only](#) [Author and Title](#)

Chelysheva L, Diallo S, Vezon D, Gendrot G, Vrielynck N, Belcram K, Rocques N, Márquez-Lema A, Bhatt AM, Horlow C, et al. (2005) *AtREC8* and *AtSCC3* are essential to the monopolar orientation of the kinetochores during meiosis. *J Cell Sci* 118: 4621-32

Pubmed: [Author and Title](#)

CrossRef: [Author and Title](#)

Google Scholar: [Author Only](#) [Title Only](#) [Author and Title](#)

Chelysheva L, Gendrot G, Vezon D, Doutriaux M-P, Mercier R, Grelon M (2007) *Zip4/Spo22* is required for class I CO formation but not for synapsis completion in *Arabidopsis thaliana*. *PLoS Genet* 3: e83

Pubmed: [Author and Title](#)

CrossRef: [Author and Title](#)

Google Scholar: [Author Only](#) [Title Only](#) [Author and Title](#)

Chelysheva L, Vezon D, Chambon A, Gendrot G, Pereira L, Lemhemdi A, Vrielynck N, Le Guin S, Novatchkova M, Grelon M (2012) The

Arabidopsis HEI10 is a new ZMM protein related to Zip3. PLoS Genet 8: e1002799

Pubmed: [Author and Title](#)

CrossRef: [Author and Title](#)

Google Scholar: [Author Only](#) [Title Only](#) [Author and Title](#)

Cromer L, Jolivet S, Horlow C, Chelysheva L, Heyman J, De Jaeger G, Koncz C, De Veylder L, Mercier R (2013) Centromeric cohesion is protected twice at meiosis, by SHUGOSHINs at anaphase I and by PATRONUS at interkinesis. Curr Biol 23: 2090-9

Pubmed: [Author and Title](#)

CrossRef: [Author and Title](#)

Google Scholar: [Author Only](#) [Title Only](#) [Author and Title](#)

Ferdous M, Higgins JD, Osman K, Lambing C, Roitinger E, Mechtler K, Armstrong SJ, Perry R, Pradillo M, Cuñado N, et al. (2012) Inter-homolog crossing-over and synapsis in Arabidopsis meiosis are dependent on the chromosome axis protein AtASY3. PLoS Genet 8: e1002507

Pubmed: [Author and Title](#)

CrossRef: [Author and Title](#)

Google Scholar: [Author Only](#) [Title Only](#) [Author and Title](#)

Fraune J, Brochier-Armanet C, Alsheimer M, Voff J-N, Schücker K, Benavente R (2016) Evolutionary history of the mammalian synaptonemal complex. Chromosoma 125: 355-60

Pubmed: [Author and Title](#)

CrossRef: [Author and Title](#)

Google Scholar: [Author Only](#) [Title Only](#) [Author and Title](#)

Higgins JD, Sanchez-Moran E, Armstrong SJ, Jones GH, Franklin FCH (2005) The Arabidopsis synaptonemal complex protein ZYP1 is required for chromosome synapsis and normal fidelity of crossing over. Genes Dev 19: 2488-500

Pubmed: [Author and Title](#)

CrossRef: [Author and Title](#)

Google Scholar: [Author Only](#) [Title Only](#) [Author and Title](#)

Higgins JD, Vignard J, Mercier R, Pugh AG, Franklin FCH, Jones GH (2008) AtMSH5 partners AtMSH4 in the class I meiotic crossover pathway in Arabidopsis thaliana, but is not required for synapsis. Plant J 55: 28-39

Pubmed: [Author and Title](#)

CrossRef: [Author and Title](#)

Google Scholar: [Author Only](#) [Title Only](#) [Author and Title](#)

Hu C-D, Chinenov Y, Kerppola TK (2002) Visualization of interactions among bZIP and Rel family proteins in living cells using bimolecular fluorescence complementation. Mol Cell 9: 789-98

Pubmed: [Author and Title](#)

CrossRef: [Author and Title](#)

Google Scholar: [Author Only](#) [Title Only](#) [Author and Title](#)

Jahns MT, Vezon D, Chambon A, Pereira L, Falque M, Martin OC, Chelysheva L, Grelon M (2014) Crossover localisation is regulated by the neddylation posttranslational regulatory pathway. PLoS Biol 12: e1001930

Pubmed: [Author and Title](#)

CrossRef: [Author and Title](#)

Google Scholar: [Author Only](#) [Title Only](#) [Author and Title](#)

Lambing C, Franklin FCH, Wang C-JR (2017) Understanding and Manipulating Meiotic Recombination in Plants. Plant Physiol 173: 1530-1542

Pubmed: [Author and Title](#)

CrossRef: [Author and Title](#)

Google Scholar: [Author Only](#) [Title Only](#) [Author and Title](#)

Lambing C, Osman K, Nuntasontorn K, West A, Higgins JD, Copenhaver GP, Yang J, Armstrong SJ, Mechtler K, Roitinger E, et al. (2015) Arabidopsis PCH2 Mediates Meiotic Chromosome Remodeling and Maturation of Crossovers. PLoS Genet 11: e1005372

Pubmed: [Author and Title](#)

CrossRef: [Author and Title](#)

Google Scholar: [Author Only](#) [Title Only](#) [Author and Title](#)

Lee DH, Kao Y-H, Ku J-C, Lin C-Y, Meeley R, Jan Y-S, Wang C-JR (2015) The Axial Element Protein DESYNAPTIC2 Mediates Meiotic Double-Strand Break Formation and Synaptonemal Complex Assembly in Maize. Plant Cell 27: 2516-29

Pubmed: [Author and Title](#)

CrossRef: [Author and Title](#)

Google Scholar: [Author Only](#) [Title Only](#) [Author and Title](#)

Malkova A, Swanson J, German M, McCusker JH, Housworth EA, Stahl FW, Haber JE (2004) Gene conversion and crossing over along the 405-kb left arm of Saccharomyces cerevisiae chromosome VII. Genetics 168: 49-63

Pubmed: [Author and Title](#)

CrossRef: [Author and Title](#)

Google Scholar: [Author Only](#) [Title Only](#) [Author and Title](#)

Martin K, Kopperud K, Chakrabarty R, Banerjee R, Brooks R, Goodin MM (2009) Transient expression in Nicotiana benthamiana fluorescent marker lines provides enhanced definition of protein localization, movement and interactions in planta. Plant J 59: 150-62

Pubmed: [Author and Title](#)

CrossRef: [Author and Title](#)
Google Scholar: [Author Only Title Only Author and Title](#)

Mercier R, Mézard C, Jenczewski E, Macaisne N, Grelon M (2015) The molecular biology of meiosis in plants. *Annu Rev Plant Biol* 66: 297-327

Pubmed: [Author and Title](#)
CrossRef: [Author and Title](#)
Google Scholar: [Author Only Title Only Author and Title](#)

Murashige T, Skoog F (1962) A Revised Medium for Rapid Growth and Bio Assays with Tobacco Tissue Cultures. *Physiol Plant* 15: 473-497

Pubmed: [Author and Title](#)
CrossRef: [Author and Title](#)
Google Scholar: [Author Only Title Only Author and Title](#)

Offenberg HH, Schalk JAC, Meuwissen RLJ, van Alderen M, Kester HA, Dietrich AJJ, Heyting C (1998) SCP2: a major protein component of the axial elements of synaptonemal complexes of the rat. *Nucleic Acids Res* 26: 2572-9

Pubmed: [Author and Title](#)
CrossRef: [Author and Title](#)
Google Scholar: [Author Only Title Only Author and Title](#)

Panizza S, Mendoza MA, Berlinger M, Huang L, Nicolas A, Shirahige K, Klein F (2011) Spo11-accessory proteins link double-strand break sites to the chromosome axis in early meiotic recombination. *Cell* 146: 372-83

Pubmed: [Author and Title](#)
CrossRef: [Author and Title](#)
Google Scholar: [Author Only Title Only Author and Title](#)

Pattabiraman D, Roelens B, Woglar A, Villeneuve AM (2017) Meiotic recombination modulates the structure and dynamics of the synaptonemal complex during *C. elegans* meiosis. *PLoS Genet* 13: e1006670

Pubmed: [Author and Title](#)
CrossRef: [Author and Title](#)
Google Scholar: [Author Only Title Only Author and Title](#)

Pelttari J, Hoja M, Yuan L, Liu J, Brundell E, Moens P, Santucci-Darmanin S, Jessberger R, Barbero JL, Heyting C, et al. (2001) A Meiotic Chromosomal Core Consisting of Cohesin Complex Proteins Recruits DNA Recombination Proteins and Promotes Synapsis in the Absence of an Axial Element in Mammalian Meiotic Cells. *Mol Cell Biol* 21: 5667-5677

Pubmed: [Author and Title](#)
CrossRef: [Author and Title](#)
Google Scholar: [Author Only Title Only Author and Title](#)

Ríos G, Lossow A, Hertel B, Breuer F, Schaefer S, Broich M, Kleinow T, Jásik J, Winter J, Ferrando A, et al. (2002) Rapid identification of *Arabidopsis* insertion mutants by non-radioactive detection of T-DNA tagged genes. *Plant J* 32: 243-53

Pubmed: [Author and Title](#)
CrossRef: [Author and Title](#)
Google Scholar: [Author Only Title Only Author and Title](#)

Ross KJ, Franz P, Armstrong SJ, Vizir I, Mulligan B, Franklin FCH, Jones GH (1997) Cytological characterization of four meiotic mutants of *Arabidopsis* isolated from T-DNA-transformed lines. *Chromosome Res* 5: 551-9

Pubmed: [Author and Title](#)
CrossRef: [Author and Title](#)
Google Scholar: [Author Only Title Only Author and Title](#)

Ross KJ, Franz P, Jones GH (1996) A light microscopic atlas of meiosis in *Arabidopsis thaliana*. *Chromosome Res* 4: 507-16

Pubmed: [Author and Title](#)
CrossRef: [Author and Title](#)
Google Scholar: [Author Only Title Only Author and Title](#)

Rossignol P, Collier S, Bush M, Shaw P, Doonan JH (2007) *Arabidopsis* POT1A interacts with TERT-V(18), an N-terminal splicing variant of telomerase. *J Cell Sci* 120: 3678-87

Pubmed: [Author and Title](#)
CrossRef: [Author and Title](#)
Google Scholar: [Author Only Title Only Author and Title](#)

Sanchez-Moran E, Santos J-L, Jones GH, Franklin FCH (2007) ASY1 mediates AtDMC1-dependent interhomolog recombination during meiosis in *Arabidopsis*. *Genes Dev* 21: 2220-33

Pubmed: [Author and Title](#)
CrossRef: [Author and Title](#)
Google Scholar: [Author Only Title Only Author and Title](#)

Schalk JA, Dietrich AJ, Vink AC, Offenberg HH, van Alderen M, Heyting C (1998) Localization of SCP2 and SCP3 protein molecules within synaptonemal complexes of the rat. *Chromosoma* 107: 540-8

Pubmed: [Author and Title](#)
CrossRef: [Author and Title](#)
Google Scholar: [Author Only Title Only Author and Title](#)

Scholl RL, May ST, Ware DH (2000) Seed and molecular resources for *Arabidopsis*. *Plant Physiol* 124: 1477-80

Pubmed: [Author and Title](#)
CrossRef: [Author and Title](#)
Google Scholar: [Author Only](#) [Title Only](#) [Author and Title](#)

Snow R (1979) Maximum Likelihood Estimation Of Linkage And Interference From Tetrad Data. Genetics 92: 231-245

Pubmed: [Author and Title](#)
CrossRef: [Author and Title](#)
Google Scholar: [Author Only](#) [Title Only](#) [Author and Title](#)

Snowden T, Acharya S, Butz C, Berardini M, Fishel R (2004) hMSH4-hMSH5 recognizes Holliday Junctions and forms a meiosis-specific sliding clamp that embraces homologous chromosomes. Mol Cell 15: 437-51

Pubmed: [Author and Title](#)
CrossRef: [Author and Title](#)
Google Scholar: [Author Only](#) [Title Only](#) [Author and Title](#)

Sun X, Huang L, Markowitz TE, Blitzblau HG, Chen D, Klein F, Hochwagen A (2015) Transcription dynamically patterns the meiotic chromosome-axis interface. Elife 4: 1-23

Pubmed: [Author and Title](#)
CrossRef: [Author and Title](#)
Google Scholar: [Author Only](#) [Title Only](#) [Author and Title](#)

Syrjänen JL, Heller I, Candelli A, Davies OR, Peterman EJG, Wuite GJL, Pellegrini L (2017) Single-molecule observation of DNA compaction by meiotic protein SYCP3. Elife 6: 1-14

Pubmed: [Author and Title](#)
CrossRef: [Author and Title](#)
Google Scholar: [Author Only](#) [Title Only](#) [Author and Title](#)

Syrjänen JL, Pellegrini L, Davies OR (2014) A molecular model for the role of SYCP3 in meiotic chromosome organisation. Elife 3: 1-18

Pubmed: [Author and Title](#)
CrossRef: [Author and Title](#)
Google Scholar: [Author Only](#) [Title Only](#) [Author and Title](#)

Vignard J, Siwiec T, Chelysheva L, Vrielynck N, Gonord F, Armstrong SJ, Schlögelhofer P, Mercier R (2007) The interplay of RecA-related proteins and the MND1-HOP2 complex during meiosis in Arabidopsis thaliana. PLoS Genet 3: 1894-906

Pubmed: [Author and Title](#)
CrossRef: [Author and Title](#)
Google Scholar: [Author Only](#) [Title Only](#) [Author and Title](#)

Vrielynck N, Chambon A, Vezon D, Pereira L, Chelysheva L, De Muyt A, Mézard C, Mayer C, Grelon M (2016) A DNA topoisomerase VI-like complex initiates meiotic recombination. Science 351: 939-43

Pubmed: [Author and Title](#)
CrossRef: [Author and Title](#)
Google Scholar: [Author Only](#) [Title Only](#) [Author and Title](#)

Wang K, Wang M, Tang D, Shen Y, Qin B, Li M, Cheng Z (2011) PAIR3, an axis-associated protein, is essential for the recruitment of recombination elements onto meiotic chromosomes in rice. Mol Biol Cell 22: 12-9

Pubmed: [Author and Title](#)
CrossRef: [Author and Title](#)
Google Scholar: [Author Only](#) [Title Only](#) [Author and Title](#)

Wojtasz L, Daniel K, Roig I, Bolcun-Filas E, Xu H, Boonsanay V, Eckmann CR, Cooke HJ, Jasin M, Keeney S, et al. (2009) Mouse HORMAD1 and HORMAD2, two conserved meiotic chromosomal proteins, are depleted from synapsed chromosome axes with the help of TRIP13 AAA-ATPase. PLoS Genet 5: e1000702

Pubmed: [Author and Title](#)
CrossRef: [Author and Title](#)
Google Scholar: [Author Only](#) [Title Only](#) [Author and Title](#)

Yang F, De La Fuente R, Leu NA, Baumann C, McLaughlin KJ, Wang PJ (2006) Mouse SYCP2 is required for synaptonemal complex assembly and chromosomal synapsis during male meiosis. J Cell Biol 173: 497-507

Pubmed: [Author and Title](#)
CrossRef: [Author and Title](#)
Google Scholar: [Author Only](#) [Title Only](#) [Author and Title](#)

Yuan L, Pelttari J, Brundell E, Björkroth B, Zhao J, Liu JG, Brismar H, Daneshmandi B, Höög C (1998) The synaptonemal complex protein SCP3 can form multistranded, cross-striated fibers in vivo. J Cell Biol 142: 331-9

Pubmed: [Author and Title](#)
CrossRef: [Author and Title](#)
Google Scholar: [Author Only](#) [Title Only](#) [Author and Title](#)

Zickler D, Kleckner N (1999) Meiotic chromosomes: integrating structure and function. Annu Rev Genet 33: 603-754

Pubmed: [Author and Title](#)
CrossRef: [Author and Title](#)
Google Scholar: [Author Only](#) [Title Only](#) [Author and Title](#)